

# A Revisit to the Hicks' Hyperbolic Two-pressure Two-phase Flow Model

The 17th International Topical Meeting on  
Nuclear Reactor Thermal Hydraulics  
(NURETH-17)

Ling Zou, Haihua Zhao, Hongbin Zhang,  
Caleb S. Brooks

January 2017

This is a preprint of a paper intended for publication in a journal or proceedings. Since changes may be made before publication, this preprint should not be cited or reproduced without permission of the author. This document was prepared as an account of work sponsored by an agency of the United States Government. Neither the United States Government nor any agency thereof, or any of their employees, makes any warranty, expressed or implied, or assumes any legal liability or responsibility for any third party's use, or the results of such use, of any information, apparatus, product or process disclosed in this report, or represents that its use by such third party would not infringe privately owned rights. The views expressed in this paper are not necessarily those of the United States Government or the sponsoring agency.

The INL is a  
U.S. Department of Energy  
National Laboratory  
operated by  
Battelle Energy Alliance



# A REVISIT TO THE HICKS' HYPERBOLIC TWO-PRESSURE TWO-PHASE FLOW MODEL

**Ling Zou, Haihua Zhao, Hongbin Zhang**

Idaho National Laboratory  
P.O. Box 1625, Idaho Falls, ID 83415-3870 USA  
ling.zou@inl.gov; haihua.zhao@inl.gov; hongbin.zhang@inl.gov

**Caleb S. Brooks**

Department of Nuclear, Plasma, and Radiological Engineering  
University of Illinois at Urbana-Champaign  
Urbana, IL 61801 USA  
csbrooks@illinois.edu

## ABSTRACT

Hicks' two-phase flow model represents one of the earliest hyperbolic two-pressure two-phase flow models developed in the early 1980s. This model was developed under the separated flow condition, but could be potentially generalized for more realistic flow conditions that are of interest to reactor safety analysis (e.g., bubbly flow). This model is mathematically hyperbolic and therefore well-posed, as eigenvalues from the characteristic analysis found to be all real. Many currently popular two-pressure models are formulated similarly to Hicks' two-pressure model, with the inclusion of a void fraction transport equation. The void fraction transport equation is closed using the knowledge of transverse velocity on the two-phase interface, which is assumed to be the solution of a Riemann problem in the transverse direction. Numerical experiments on two phenomenological test problems, i.e., the two-phase water faucet problem and the sedimentation problem, were performed using the Hicks' model, as well as the single-pressure two-phase flow model. Numerical results demonstrate that the channel size, which appears in the void fraction transport equation, has significant impact on the behavior of the Hicks' model. By comparing to single-pressure model results and available analytical solutions, it was found that Hicks' model with very small channel width behaves similarly to the single-pressure model. On the contrary, Hicks' model with large channel width, however, constantly leads to unphysical liquid-phase pressure. These numerical experiments indicate that using the Riemann problem to close the equation system in Hicks' derivation might be a questionable approach. Further investigations are necessary to explore different approaches that will properly close the equation system without leading to unphysical behaviors.

KEYWORDS

Hyperbolic, Two-pressure, Two-phase flow model

## 1 Introduction

It is a well-known fact that many of the single-pressure two-phase flow equations systems possess complex-valued characteristics and hence are ill-posed [1]. In the past, different treatments have been proposed and implemented to resolve this issue in system analysis codes. For example, a virtual mass term in the RELAP5 code [2] and an interfacial pressure treatment in the CATHARE code [3] are used to render the equation system hyperbolic. In recent years, there are renewed interest in hyperbolic two-pressure two-phase flow models in the nuclear thermal-hydraulics field [4, 5]. The development of such hyperbolic two-pressure two-phase flow models could date back to the 1970s. The first documented hyperbolic two-pressure two-phase flow model probably attributed to Ransom

and co-workers [6], in which a simple separated flow condition was considered. It is probable that Hicks [7] independently developed a similar model under the separated flow condition in 1981, which also provided discussions on model extension to more general conditions. Both Ransom's and Hicks' models were later published in 1984 as a united model [8]. Later, in 1986, Baer and Nunziato proposed a hyperbolic two-pressure two-phase flow model to describe the deflagration-to-detonation transition (DDT) in reactive granular materials [9]. Similar to Ransom and Hicks' approach in closing the model, Baer and Nunziato introduced a volume fraction transport equation for the less compressible solid phase. Baer and Nunziato's model later became popular and has impacted many currently active two-phase flow researches, e.g., [10] and [11]. However, it is interesting to observe that most of these models [10, 11] closely resemble the Hicks' two-pressure model. It is the objective of this paper to revisit the Hicks' two-pressure five-equation two-phase flow model, herein referred as the 5E2P model. By exploring several properties of this simple yet complete model, we are hoping that insights could be gained towards many two-pressure two-phase flow models that are currently used in the nuclear reactor thermal-hydraulics field.

## 2 Model Descriptions

Hicks' two-pressure two-phase flow model, i.e., the 5E2P model, consists of a transport equation for the volume fraction, two mass conservation equations, and two momentum conservation equations. Following notations used in [8], these five equations are given as follows,

$$\frac{\partial \alpha_1}{\partial t} + \hat{u} \frac{\partial \alpha_1}{\partial x} - \frac{\hat{v}}{H} = 0 \quad (1)$$

$$\frac{\partial \alpha_1 \rho_1}{\partial t} + \frac{\partial \alpha_1 \rho_1 u_1}{\partial x} = 0 \quad (2)$$

$$\frac{\partial \alpha_1 \rho_1 u_1}{\partial t} + \frac{\partial \alpha_1 \rho_1 u_1^2}{\partial x} + \alpha_1 \frac{\partial p_1}{\partial x} + (p_1 - \hat{p}) \frac{\partial \alpha_1}{\partial x} - \alpha_1 \rho_1 g = 0 \quad (3)$$

$$\frac{\partial (1 - \alpha_1) \rho_2}{\partial t} + \frac{\partial (1 - \alpha_1) \rho_2 u_2}{\partial x} = 0 \quad (4)$$

$$\frac{\partial (1 - \alpha_1) \rho_2 u_2}{\partial t} + \frac{\partial (1 - \alpha_1) \rho_2 u_2^2}{\partial x} + (1 - \alpha_1) \frac{\partial p_2}{\partial x} + (p_2 - \hat{p}) \frac{\partial (1 - \alpha_1)}{\partial x} - (1 - \alpha_1) \rho_2 g = 0 \quad (5)$$

where  $\alpha_1$ ,  $p_{1,2}$ ,  $u_{1,2}$  are the primary nonlinear variables, representing volume fraction of phase 1, pressures of phase 1 and 2, and axial velocities of phase 1 and 2, respectively. The equation system is closed by introducing equation of state and additional closures for quantities at the two-phase interface, e.g.,  $\hat{u}$ ,  $\hat{v}$ , and  $\hat{p}$ . For barotropic fluid, the phasic density is determined from the equation of state as,  $\rho_k = \rho_k(p_k)$ . For  $\hat{u}$ , Hicks suggested that [7],  $\hat{u} = \alpha_1 u_1 + \alpha_2 u_2$ . It was also suggested that  $\hat{v}$  and  $\hat{p}$  could be found as solutions to a Riemann problem in the transverse direction, which resulted,

$$\hat{v} = \frac{p_1 - p_2}{a_1 + a_2}, \quad (6)$$

and

$$\hat{p} = \frac{p_1/a_1 + p_2/a_2}{1/a_1 + 1/a_2}, \quad (7)$$

where  $a_k$  is the acoustic impedance of phase  $k$ , which is defined as  $a_k = \rho_k c_k$ , and  $c_k$  is the sound speed of phase  $k$  that is defined as  $c_k^2 = dp_k/d\rho_k$ .

## 2.1 Characteristic Analysis

This section discusses the hyperbolic property of the 5E2P equation system, which has been provided in both [7] and [8]. This section is included for the purpose of completeness. Let  $\bar{\rho}_1 \equiv \alpha_1 \rho_1$ ,  $\bar{\rho}_2 \equiv (1 - \alpha_1) \rho_2$ ,  $\bar{m}_1 \equiv \alpha_1 \rho_1 u_1$ , and  $\bar{m}_2 \equiv (1 - \alpha_1) \rho_2 u_2$ . Using equation of state  $p_1 = p_1(\rho_1) = p_1(\bar{\rho}_1/\alpha_1)$ , apply chain rule,

$$\frac{\partial p_1}{\partial x} = \frac{dp_1}{d\rho_1} \frac{\partial}{\partial x} \left( \frac{\bar{\rho}_1}{\alpha_1} \right) = c_1^2 \left( \frac{1}{\alpha_1} \frac{\partial \bar{\rho}_1}{\partial x} - \frac{\bar{\rho}_1}{\alpha_1^2} \frac{\partial \alpha_1}{\partial x} \right) \quad (8)$$

Similar derivations can be done for  $p_2$ , and the original set of equation could be expressed as,

$$\frac{\partial \bar{\rho}_1}{\partial t} + \frac{\partial \bar{m}_1}{\partial x} = 0 \quad (9)$$

$$\frac{\partial \bar{m}_1}{\partial t} + (c_1^2 - u_1^2) \frac{\partial \bar{\rho}_1}{\partial x} + 2u_1 \frac{\partial \bar{m}_1}{\partial x} + \mathcal{P}_1 \frac{\partial \alpha_1}{\partial x} - \bar{\rho}_1 g = 0 \quad (10)$$

$$\frac{\partial \bar{\rho}_2}{\partial t} + \frac{\partial \bar{m}_2}{\partial x} = 0 \quad (11)$$

$$\frac{\partial \bar{m}_2}{\partial t} + (c_2^2 - u_2^2) \frac{\partial \bar{\rho}_2}{\partial x} + 2u_2 \frac{\partial \bar{m}_2}{\partial x} - \mathcal{P}_2 \frac{\partial \alpha_2}{\partial x} - \bar{\rho}_2 g = 0 \quad (12)$$

$$\frac{\partial \alpha_1}{\partial t} + \hat{u} \frac{\partial \alpha_1}{\partial x} - \frac{\hat{v}}{H} = 0 \quad (1)$$

where  $\mathcal{P}_k = p_k - \hat{p} - \rho_k c_k^2$ , with  $k = (1, 2)$ . This set of equation can be re-written in the vector form,

$$\frac{\partial \mathbf{U}}{\partial t} + \mathbb{A}(\mathbf{U}) \frac{\partial \mathbf{U}}{\partial x} + \mathbf{d}(\mathbf{U}) = 0 \quad (13)$$

where  $\mathbf{U} = [\bar{\rho}_1, \bar{m}_1, \bar{\rho}_2, \bar{m}_2, \alpha_1]^T$ , and,

$$\mathbb{A}(\mathbf{U}) = \begin{bmatrix} 0 & 1 & 0 & 0 & 0 \\ c_1^2 - u_1^2 & 2u_1 & 0 & 0 & \mathcal{P}_1 \\ 0 & 0 & 0 & 1 & 0 \\ 0 & 0 & c_2^2 - u_2^2 & 2u_2 & -\mathcal{P}_2 \\ 0 & 0 & 0 & 0 & \hat{u} \end{bmatrix} \quad (14)$$

$$\mathbf{d}(\mathbf{U}) = [0, -\bar{\rho}_1 g, 0, -\bar{\rho}_2 g, -\hat{v}/H]^T \quad (15)$$

Characteristic analysis for the two-pressure model can be performed by finding the roots of the characteristic polynomial resulting from,

$$\det(\lambda \mathbb{I} - \mathbb{A}) = 0 \quad (16)$$

which can be written explicitly as,

$$P_5(\lambda) \equiv \det \begin{bmatrix} \lambda & -1 & 0 & 0 & 0 \\ -c_1^2 + u_1^2 & \lambda - 2u_1 & 0 & 0 & -\mathcal{P}_1 \\ 0 & 0 & \lambda & 1 & 0 \\ 0 & 0 & -c_2^2 + u_2^2 & \lambda - 2u_2 & \mathcal{P}_2 \\ 0 & 0 & 0 & 0 & \lambda - \hat{u} \end{bmatrix} = 0 \quad (17)$$

and it can be manipulated to obtain,

$$P_5(\lambda) = [(\lambda - u_1)^2 - c_1^2][(\lambda - u_2)^2 - c_2^2](\lambda - \hat{u}) \quad (18)$$

It is easily found that the five roots are,

$$\lambda = \hat{u}, u_1 \pm c_1, u_2 \pm c_2. \quad (19)$$

which are all real values for all physically acceptable states, and thus the two-pressure two-phase flow model is hyperbolic and well-posed.

## 2.2 Discussions on Single-phase Condition

Any two-phase flow equation has to model correctly the single-phase condition where void fraction is zero or one. Phase appearance and disappearance are also great challenges to numerical simulations, because normally the set of equations associated to the disappearing phase would also vanish. Before numerical experiments are carried out, several discussions are provided here on what needs to be done to address such an issue, as well as what should be expected from numerical results. For the 5E2P model, taking  $\alpha_1 = 0$  as an example, we concluded that any valid solution to equation (1) with closure equation (6) has to satisfy,

$$p_1 = p_2 \quad (20)$$

In addition, at the single-phase condition of  $\alpha_1 = 0$ , the momentum equation of phase 1, e.g., equation (3), admits infinitely many solutions to the velocity of phase 1. Similarly, it applies to phase 2, when  $\alpha_1 = 1$ . As discussed in a previous paper [12], this issue can be resolved by introducing a drag term in the momentum equation, taking the form of,

$$F_{int} = C_i(u_1 - u_2) \quad (21)$$

where  $C_i$  is the drag coefficient. In this paper, the drag coefficient  $C_i$  is modeled with a similar approach used in [12]. Numerically,  $C_i$  is computed the normal way when void fraction are not close to 0 (or 1); while it is computed as a non-zero finite value when the void fraction is close to 0 (or 1). For more details, readers are referred to [12].

## 3 Numerical Experiments

Numerical experiments are carried out on two phenomenological test cases, i.e., the classical water faucet problem and two-phase separation problem (also known as sedimentation problem). In this section, numerical results will be obtained with different  $(1/H)$  values, and the effect of  $(1/H)$  will then be explored. Analytical solutions and numerical results from single-pressure two-phase flow model will also be presented for comparisons.

### 3.1 Numerical methods

In this paper, numerical methods are only discussed briefly. For spatial discretization, first-order donor-cell type of upwind method is applied on staggered-grid mesh arrangement. Momentum equations are simplified in their primitive forms and are reorganized for numerical convenience. For example, equation (3) is written as,

$$\alpha_1 \rho_1 \frac{\partial u_1}{\partial t} + \alpha_1 \rho_1 u_1 \frac{\partial u_1}{\partial x} + \frac{\partial \alpha_1 p_1}{\partial x} - \hat{p} \frac{\partial \alpha_1}{\partial x} - \alpha_1 \rho_1 g = 0 \quad (22)$$

Note that the additional drag term is included for the sedimentation problem because single-phase condition is evolved due to phase separation. The drag term is turned off for the water faucet problem following the problem setting. Similarly, the void fraction equation is rewritten for numerical convenience,

$$\frac{\partial \alpha_1}{\partial t} + \frac{\partial \alpha_1 \hat{u}}{\partial x} - \alpha_1 \frac{\partial \hat{u}}{\partial x} - \frac{\hat{v}}{H} = 0 \quad (23)$$

For staggered-grid mesh,  $\alpha_k$ ,  $p_k$ ,  $\rho_k$ ,  $\hat{v}$ , and  $\hat{p}$  are arranged on cell centers, while  $u_k$  and  $\hat{u}$  are arranged on cell edges. For time integration scheme, the standard Backward Euler (BDF1) scheme is used. The discretized nonlinear equation system is solved with a Jacobian-free Newton Krylove (JFNK) method. More details on numerical discretization and the JFNK method are referred to our previous papers [13, 14].

### 3.2 Water faucet problem

Originally proposed by Ransom [15], the one-dimensional water faucet problem has been widely used as a benchmark problem in two-phase flow studies. The problem consists of a vertical pipe with length  $L = 12m$ . Initially, the pipe is partially filled with a uniform column of liquid ( $\alpha_l = 0.8$ ) and gas ( $\alpha_g = 0.2$ ). Hereafter, the subscripts ‘ $l$ ’ and ‘ $2$ ’, ‘ $g$ ’ and ‘ $1$ ’ will be used interchangeably. Initially, the liquid column moving at  $u_{l,init} = 10m/s$ , and the gas phase stays still at  $u_{g,init} = 0m/s$ . Analytical solutions to this problem were provided by Ransom in [15], with extensions to this Ransom’s solutions discussed in [14].

Transient and steady-state numerical results were obtained for different  $(1/H)$  values for the water faucet problem, e.g.,  $(1/H) = 20000$  in figure 1,  $(1/H) = 2000$  in figure 2, and so on, till  $(1/H) = 2$  in figure 5. Correspondingly, the channel widths for these cases are  $H = 10^{-4}m$ ,  $H = 10^{-3}m$ , ...,  $H = 1.0m$ . It is noted that a two-layer effect discussed in the end of section 1.2 of [7] has been considered. Numerical results were also obtained for the single-pressure two-phase flow model as the reference results. Hereafter, the single-pressure two-phase flow model is also referred as the 4E1P model, in contrast with the two-pressure 5E2P model. For both models, numerical results were obtained using 384 finite volume cells ( $N = 384$ ) and time step size at  $\Delta t = 1.0 \times 10^{-3}s$  that corresponds to CFL = 0.8 for maximum velocity of  $\sim 25 m/s$  observed during simulations.

From figures 1 to 5, it is clear that the 5E2P model results deviate more and more from the 4E1P model results (and analytical solutions), as the value of  $(1/H)$  decreasing from 20000 to 2. As shown in figure 1, numerical results on void fraction for both the 5E2P and 4E1P models almost overlapped altogether. At the steady state, both models predict almost perfect results compared to the analytical solution. This is expected as very large  $(1/H)$  value corresponds to the instantaneous pressure relaxation procedure described in [10]. However, when the value of  $(1/H)$  decreases, numerical results from the 5E2P model change significantly, and they deviate from both the 4E1P results and analytical solutions for small  $(1/H)$  values. The liquid phase pressure for  $(1/H) = 2$  in figure 5 and  $(1/H) = 20$  in figure 4 are obviously unphysical. It might be a reasonable approach to include the channel width  $H$  in one-dimensional two-phase flow model in certain situations to include the surface tension effect [16], or the gravity effect [17]. It seems to be a questionable approach to do so in a more general manner as a way to close the equation system. As it can be expected, by including channel width  $H$  into the equation, numerical results of a presumably one-dimensional problem (e.g. the water faucet problem) now depend on the channel width. One could certainly argue that the water faucet problem or any other one-dimensional problems are truly multidimensional. The nonphysical behaviors of liquid phase pressures shown in figures 4 and 5 are strong evidences indicating that there might be fundamental flaws in the current 5E2P formulation. As the void fraction transport equation follows strict mathematical derivation,

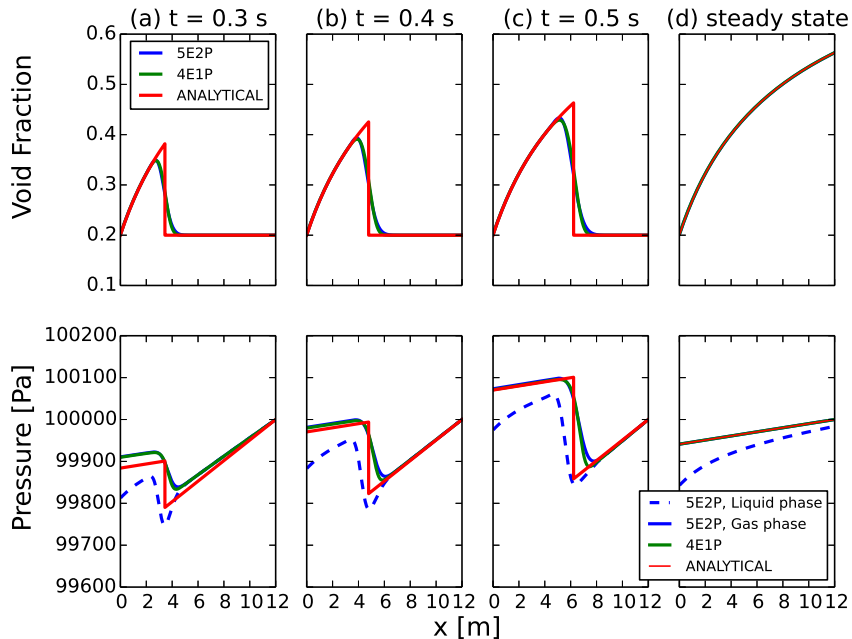


Figure 1: **Numerical results of the two-pressure model with  $1/H = 20000.0$ . All simulations are from  $N = 384$  and  $\Delta t = 1.0 \times 10^{-3}s$ .**

it is possible that using Riemann problem to close the equation system, e.g., to obtain  $\hat{v}$  and  $\hat{p}$  in terms of other *averaged* quantities, could be a problematic approach.

Numerical results were also obtained for both the 5E2P with  $1/H = 2000$  and  $20000$ , and 4E1P models with refined meshes and time step sizes. Meshes are refined to 768 (figure 6) and 1536 cells (figure 7), and the corresponding time step sizes are refined to  $5.0 \times 10^{-4}s$  and  $2.5 \times 10^{-4}s$ , respectively, so that constant  $\Delta x/\Delta t$  ratio is maintained. For the ill-posed 4E1P model, it is not surprising to observe that the numerical solutions eventually “*blow up*” as mesh refinement continues. As shown in figure 7, an uncontrollable *spike* in void fraction profile has been developed near the discontinuity front, which eventually leads to simulation failure for unphysical behavior. It is indeed a surprise to observe a similar scenario in the numerical solutions of the 5E2P model. Even for the case using 768 cells, there are unstable waves already developed with the 5E2P model ( $1/H = 2000$ ). The simulation could eventually reach steady state as these unstable waves pass through. With finer mesh using 1536 cells, the growth of these unstable waves’ magnitudes became uncontrollable, which also leads to eventual simulation failure due to unphysical behavior. The reason for such unstable wave structure developed using a well-posed system is currently unknown. Linear stability analysis that follows Ramshaw and Trapp’s approach [16] has also been performed, but unfortunately there has been not much useful information revealed.

### 3.3 Sedimentation problem

The sedimentation problem is a test problem originally proposed by Youngs [15] for testing the phase separation due to gravity effect. The test consists of a vertical pipe ( $2\text{ m}$  in length) initially filled with a two-phase mixture having a uniform void fraction  $\alpha_{init} = 0.5$ . Due to gravity effect, the two phases will eventually separate into two single-phase zones with the heavier liquid phase

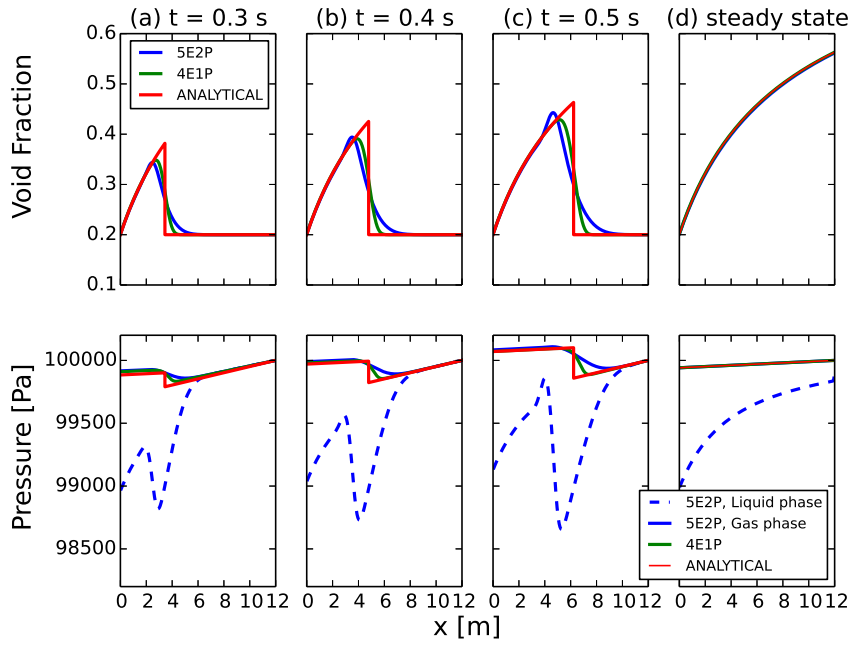


Figure 2: Numerical results of the two-pressure model with  $1/H = 2000.0$ . All simulations are from  $N = 384$  and  $\Delta t = 1.0 \times 10^{-3}s$ .

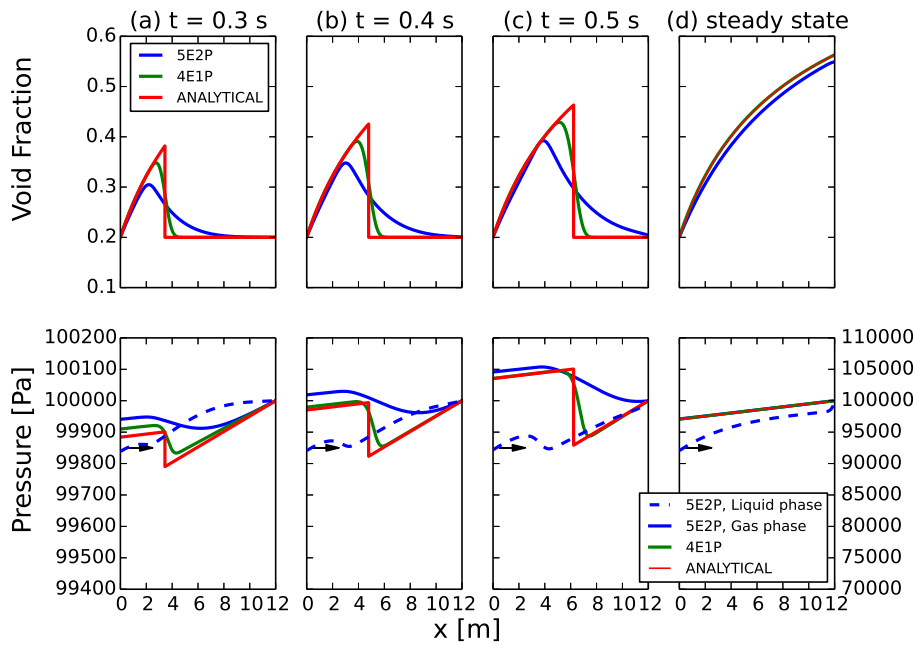


Figure 3: Numerical results of the two-pressure model with  $1/H = 200.0$ . All simulations are from  $N = 384$  and  $\Delta t = 1.0 \times 10^{-3}s$ .

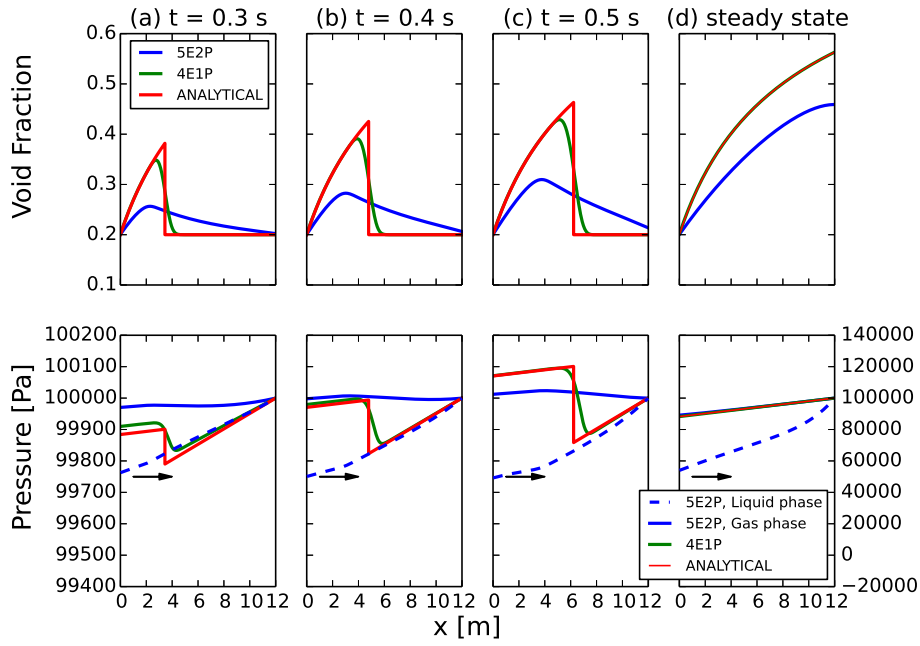


Figure 4: Numerical results of the two-pressure model with  $1/H = 20.0$ . All simulations are from  $N = 384$  and  $\Delta t = 1.0 \times 10^{-3}s$ .

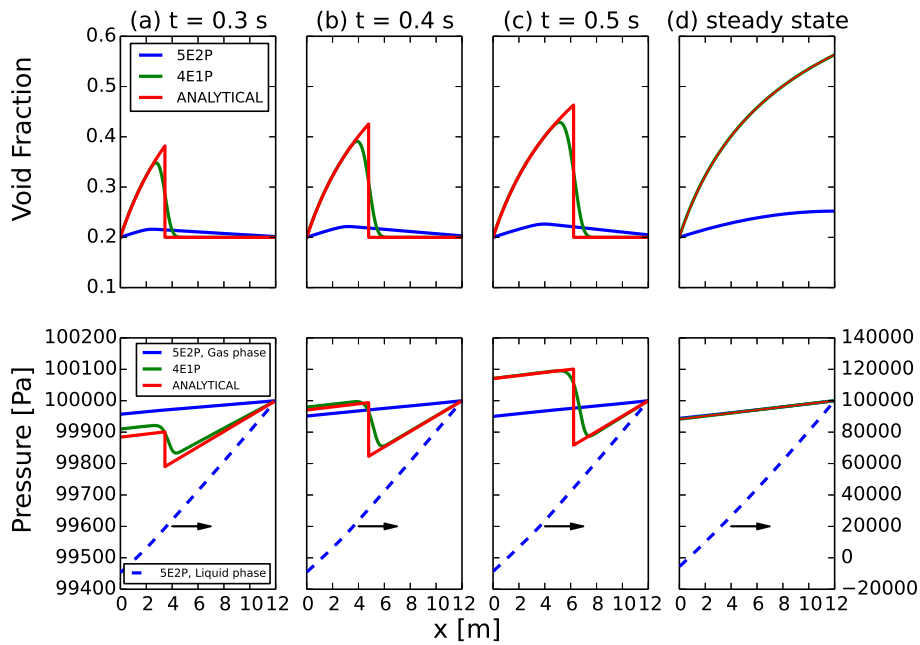


Figure 5: Numerical results of the two-pressure model with  $1/H = 2.0$ . All simulations are from  $N = 384$  and  $\Delta t = 1.0 \times 10^{-3}s$ .

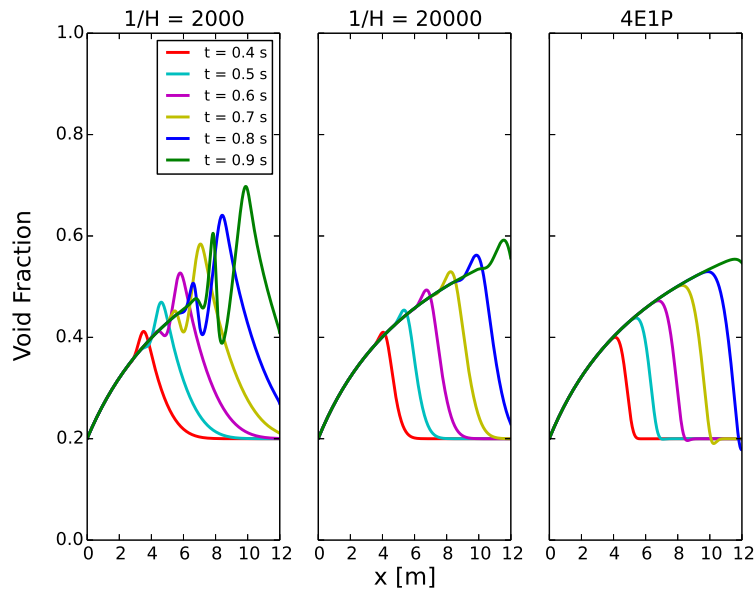


Figure 6: Numerical results of the two-pressure model with  $1/H = 2000.0$ ,  $1/H = 20000.0$ , and from the 4E1P model. All simulations are from  $N = 768$  and  $\Delta t = 5.0 \times 10^{-4} s$ .

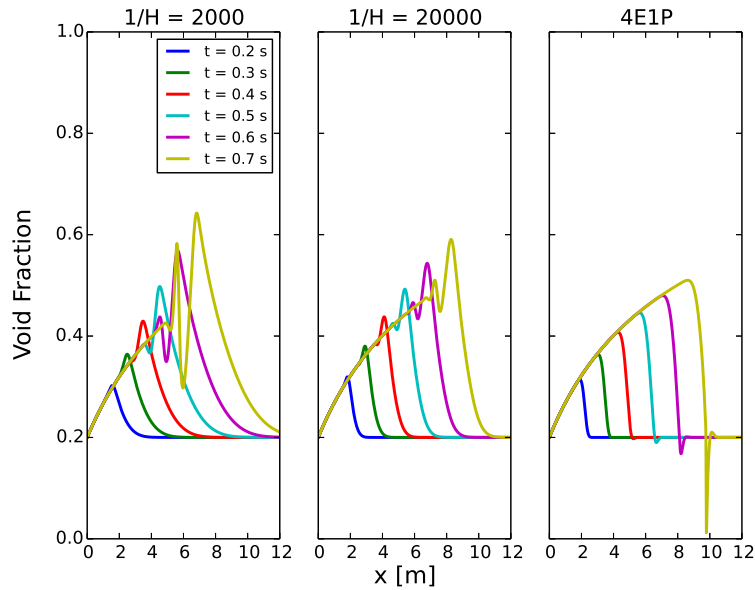


Figure 7: Numerical results of the two-pressure model with  $1/H = 2000.0$ ,  $1/H = 20000.0$ , and from the 4E1P model. All simulations are from  $N = 1536$  and  $\Delta t = 2.50 \times 10^{-4} s$ . All simulations failed at a later time due to instability that eventually causes void fraction reaches 0 or 1.

settling down at the bottom, and the lighter phase at the top of the pipe.

Similar to the water faucet problem, numerical results were obtained using the 5E2P model with different  $1/H$  values. Numerical results from the 4E1P model have also been obtained for comparison. For this particular problem, analytical solutions are not available. As shown in figure 8 (4E1P model), two discontinuous void fronts could be found to move upward and downward, and eventually merged in the center of the pipe at about 10 s. Hydrostatic pressure has also been correctly established at this point. Numerical results of the 5E2P model with different  $1/H$  values are plotted in figure 9 for  $1/H = 20000$ , figure 10 for  $1/H = 2000$ , figure 11 for  $1/H = 200$ , and figure 12 for  $1/H = 20$ , respectively. For very large  $1/H$  value of 20000 (figure 9), the 5E2P model numerical results are very close to those of the 4E1P model (figure 8). The two phasic pressures are pretty much identical due to the *instantaneous pressure relaxation* effect discussed in the previous section, and they are very close to the pressure results from 4E1P model. However, the phase separation process changes significantly as the  $1/H$  value decreasing, which is evident from the void fraction profiles at various times shown in these figures. Moreover, it takes much longer time to complete phase separation for smaller  $1/H$  values. For example, it takes about 24 s for  $1/H = 200$ , while about 70 s for  $1/H = 20$  to complete the phase separation, in contrast with 10 s for large  $1/H$  value and the 4E1P model. Similar to the water faucet problem, unphysical liquid phase pressure starts to appear as the value of  $1/H$  is reduced.

### 3.4 Discussion on unphysical liquid-phase pressure

In both numerical experiments, unphysically low liquid-phase pressure has been observed. Such unphysical behavior is probably due to the mismatch between the time rate of change of mass and volume fraction of the liquid phase (the more incompressible one). To demonstrate this, consider when a fraction of liquid phase mass leaves a control volume (e.g., a finite volume cell), its volume fraction has to change more or less proportionally for its incompressibility. In cases that its volume fraction changes slower than it should be, artificial depressurization takes places for the liquid phase due to decrease in density. The  $\hat{v}/H$  term counter-balances this effect and tends to equilibrate the two pressures. However, the timescale to equilibrate the two pressures is dictated by the value of  $1/H$ . The smaller is the value of  $1/H$ , the larger the timescale is and the slower the pressure equilibrium process is. Numerical experiments performed in this paper suggest that it is probably an inappropriate assumption using the Riemann problem solutions to close the equation system. Such an approach obviously leads to unphysical pressure equilibrium timescale as observed in this paper. In a similar two-pressure two-phase flow model, Guillard [18] suggested the response time for pressure equilibrium should be very close to zero. Saurel and Abgrall [10] also suggested that pressure relaxation should be considered instantaneous if such relaxation rate has not been physically or experimentally determined.

## 4 Conclusions

In this paper, we paid a revisit to an early two-pressure model proposed by Hicks. The model uses an additional void fraction transport equation to close the equation system with unequal phasic pressures. The void fraction transport equation requires the knowledge on transverse velocity on the two-phase interface, which is then assumed to be the solution of a Riemann problem in the transverse direction. The model is mathematically well-posed as all eigenvalues of characteristic analysis are real. Numerical experiments were performed on two phenomenological problems, i.e., the water faucet and sedimentation problems. Numerical results were compared to analytical solutions and numerical results from single-pressure two-phase flow model. It was found that

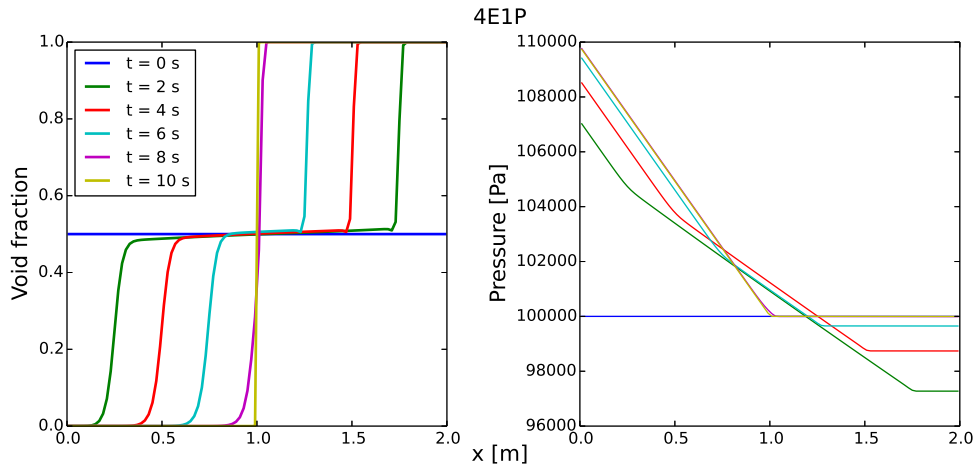


Figure 8: Numerical results of the sedimentation problem using the single-pressure **4E1P** model. Simulation was performed with  $N = 100$  and  $\Delta t = 5.0 \times 10^{-3} s$ .

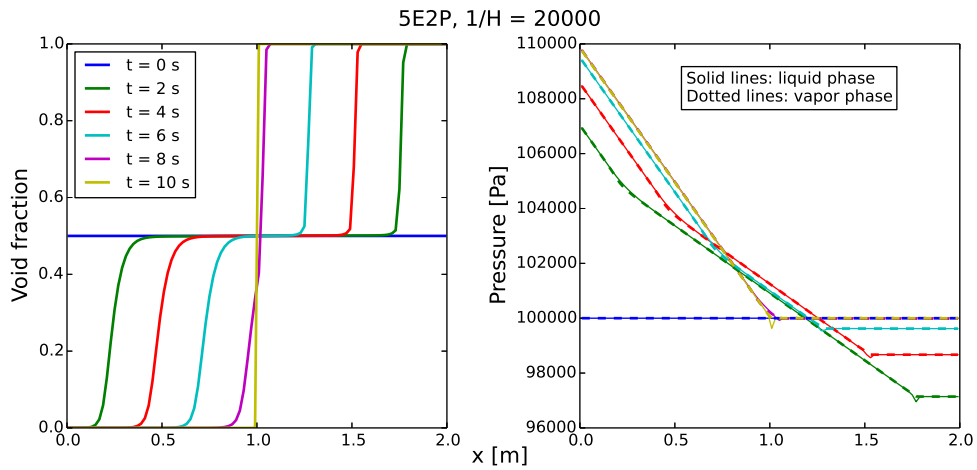


Figure 9: Numerical results of the sedimentation problem using the two-pressure **5E2P** model with  $1/H = 20000$ . Simulation was performed with  $N = 100$  and  $\Delta t = 1.0 \times 10^{-2} s$ .

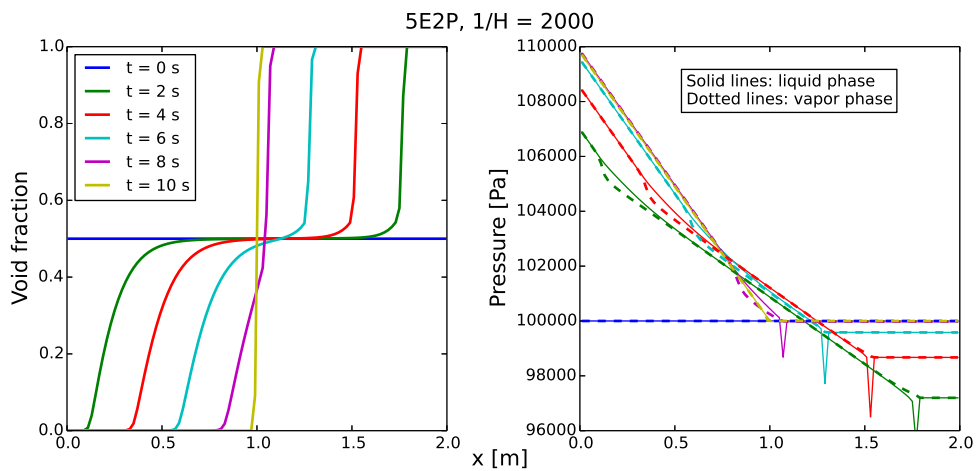


Figure 10: Numerical results of the sedimentation problem using the two-pressure 5E2P model with  $1/H = 2000$ . Simulation was performed with  $N = 100$  and  $\Delta t = 1.0 \times 10^{-2} s$ .

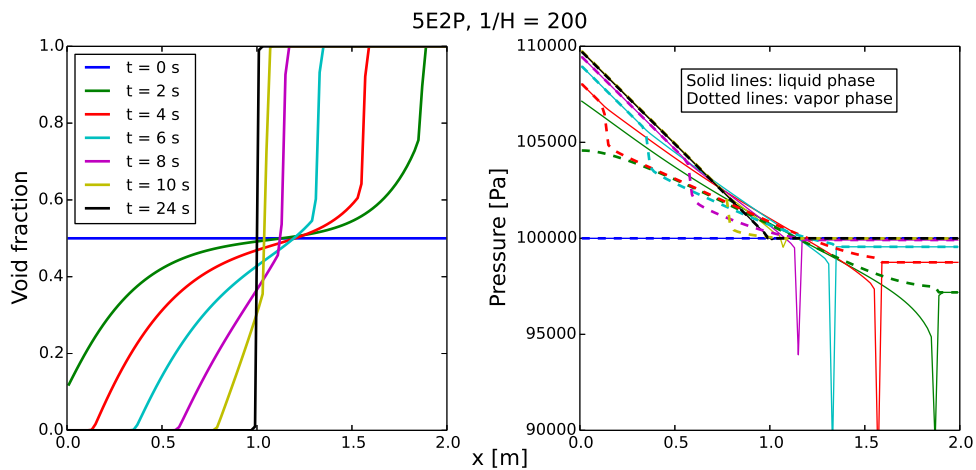


Figure 11: Numerical results of the sedimentation problem using the two-pressure 5E2P model with  $1/H = 200$ . Simulation was performed with  $N = 100$  and  $\Delta t = 5.0 \times 10^{-3} s$ .

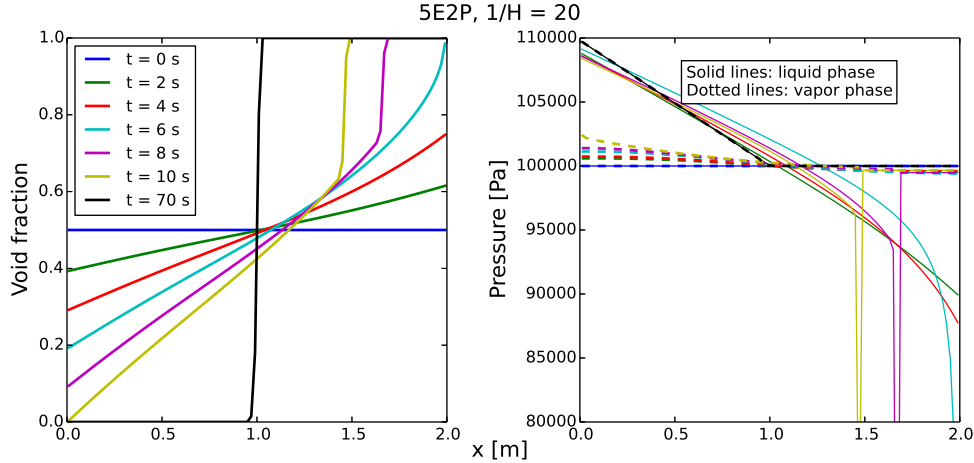


Figure 12: Numerical results of the sedimentation problem using the two-pressure 5E2P model with  $1/H = 20$ . Simulation was performed with  $N = 100$  and  $\Delta t = 5.0 \times 10^{-3} s$ .

numerical results significantly depend on the channel size, i.e., the value of  $H$ . For very large  $1/H$  values, numerical results seem to be physical and are very close to those from single-pressure model. For small  $1/H$  values, unphysical liquid-phase pressure appears, which indicates it is probably a questionable approach using Riemann problem to close the equation system. A future study is needed to investigate a method that can properly close such a two-pressure two-phase flow equation system.

## 5 Acknowledgement

This work is supported by the U.S. Department of Energy, under Department of Energy Idaho Operations Office Contract DE-AC07-05ID14517. Accordingly, the U.S. Government retains a nonexclusive, royalty-free license to publish or reproduce the published form of this contribution, or allow others to do so, for U.S. Government purposes. This work is also partially supported from the DOE NEUP funding under project number 16-10630.

## References

- [1] R.W. Lyczkowski, D. Gidaspow, C.W. Solbrig, and E.D. Hughes, "Characteristics and stability analyses of transient one-dimensional two-phase flow equations and their finite difference approximations," *Nuclear Science and Engineering* **66** (3), pp. 378-396 (1978).
- [2] "RELAP5/MOD3.3 Code Manual Volume I," NUREG/CR- 5535 ed., U.S. Nuclear Regulatory Commission, December, (2001).
- [3] D. Bestion, "The physical closure laws in the CATHARE code," *Nucl. Eng. Des.* **124** (3), pp. 229-245 (1990).
- [4] R.A. Berry, et al., "RELAP-7 theory manual," Idaho National Laboratory, INL/EXT-14-31366, 2014.

- [5] A. Guelfi, et al., “NEPTUNE: a new software platform for advanced nuclear thermal hydraulics,” *Nuclear Science and Engineering* **156** (3), pp. 281-324 (2007).
- [6] V.H. Ransom and M.P. Scofield, “Two-pressure hydrodynamic model for two-phase separated flow,” Idaho National Engineering Laboratory, SRD-50-76, 1976.
- [7] D.L. Hicks, “Hyperbolic models for two-phase (or two-material) flow,” Sandia National Laboratories, SAND-81-0253, 1981.
- [8] V.H. Ransom and D.L. Hicks, “Hyperbolic two-pressure models for two-phase flow,” *Journal of Computational Physics* **53** (1), pp. 124-151 (1984).
- [9] M. Baer and J. Nunziato, “A two-phase mixture theory for the deflagration-to-detonation transition (ddt) in reactive granular materials,” *Int. J. Multiphase Flow* **12** (6), pp. 861-889 (1986).
- [10] R. Saurel and R. Abgrall, “A multiphase Godunov method for compressible multifluid and multiphase flows,” *Journal of Computational Physics* **150** (2), pp. 425-467 (1999).
- [11] T. Gallouët, J. Hérard, and N. Seguin, “Numerical Modelling of Two-Phase Flows Using the Two-Fluid Two-Pressure Approach,” *Math. Models Methods Appl. Sci.* **14**, pp. 663-700 (2004).
- [12] L. Zou, H. Zhao, and H. Zhang, “Implicitly solving phase appearance and disappearance problems using two-fluid six-equation model,” *Progress in Nuclear Energy* **88**, pp. 198-210 (2016).
- [13] L. Zou, H. Zhao, and H. Zhang, “Application of Jacobian-free Newton-Krylov method in implicitly solving two-fluid six-equation two-phase flow problems: Implementation, validation and benchmark,” *Nuclear Engineering and Design* **300**, pp. 268-281 (2016).
- [14] L. Zou, H. Zhao, and H. Zhang, “New analytical solutions to the two-phase water faucet problem,” *Progress in Nuclear Energy* **91**, pp. 389-398 (2016).
- [15] G.F. Hewitt, J.M. Delhay, and N. Zuber, (Eds.), *Multiphase Science and Technology*, vol. 3. John Wiley & Sons Ltd, 1987.
- [16] J.D. Ramshaw and J.A. Trapp, “Characteristics, stability and short-wavelength phenomena in two-phase flow equation systems,” *Nuclear Science and Engineering* **66**, pp. 93-102 (1978).
- [17] W.D. Fullmer, V.H. Ransom, and M.A. Lopez de Bertodano, “Linear and nonlinear analysis of an unstable, but well-posed, one-dimensional two-fluid model for two-phase flow based on the inviscid Kelvin-Helmholtz instability,” *Nuclear Engineering and Design* **268**, pp. 173-184 (2014).
- [18] H. Guillard and Labois M., “Numerical modelling of compressible two-phase flows,” *Proceedings of the European conference on computational fluid dynamics (ECCOMAS CFD 2006)*, Egmond aan Zee, The Netherlands, September 5-8 (2006).